

Mean-field effects in hot and dense matter

Che-Ming Ko
Texas A&M University

- ☐ My interactions with Gerry
- ☐ Our work on medium effects in HIC
- ☐ Experimental constraints on hadronic mean fields from HIC
- ☐ Particle and antiparticle elliptic flows at RHIC
- ☐ Effects of hadronic mean fields on elliptic flow
- ☐ Effects of partonic mean fields on elliptic flow
- ☐ Implications for QCD phase diagram

Supported by National Science Foundation and the Welch Foundation

My interactions with Gerry

- 1969 - 1973:
 - Worked as Gerry's student on nuclear deformation energies
 - Published two papers in PLB and NPA
- 1990 - 1993:
 - Collaborated with Gerry on medium effects on particle production in HIC
 - Published five papers in PRL, PRC (2), PLB, ZPA
 - Graduate student Li Xiong hired by Gerry as postdoc in 1991
- 1995 – 1996:
 - Collaborated with Gerry on dilepton production in HIC
 - Published five papers in PRL, NPA (3), PLB
 - Postdoc Guo-Qiang Li hired by Gerry as postdoc in 1995
- Fall 1996:
 - Took sabbatical leave in Gerry's group and completed two review papers (JPG,ARNPS) on medium effects in HIC

Our work on mean-field effects in HIC

VOLUME 66, NUMBER 20

PHYSICAL REVIEW LETTERS

20 MAY 1991

Effect of Chiral Restoration on Kaon Production in Relativistic Heavy-Ion Collisions

C. M. Ko, Z. G. Wu, and L. H. Xia^(a)

Cyclotron Institute and Physics Department, Texas A&M University, College Station, Texas 77843

G. E. Brown

Physics Department, State University of New York, Stony Brook, Stony Brook, New York 11794

(Received 26 April 1990)

Kaon production from meson-meson annihilation is enhanced significantly because of the decrease of hadron masses in hot and dense matter as a result of the restoration of chiral symmetry. We show that this can lead to enhanced kaon yield in high-energy heavy-ion collisions.

PHYSICAL REVIEW C

VOLUME 43, NUMBER 4

APRIL 1991

Kaon production from hot and dense matter formed in heavy-ion collisions

G. E. Brown

Physics Department, State University of New York at Stony Brook, Stony Brook, New York 11794

C. M. Ko, Z. G. Wu, and L. H. Xia*

Cyclotron Institute and Physics Department, Texas A&M University, College Station, Texas 77843

(Received 19 September 1990)

In heavy-ion collisions, kaons can be produced from baryon-baryon, meson-baryon, and meson-meson interactions. Simple meson-exchange models are introduced to study kaon production from these processes in the free space. These models are then extended to determine kaon production in hot, dense nuclear matter by taking into account the decreasing hadron masses as a result of the restoration of chiral symmetry and the condensation of kaons. We find that the cross sections for kaon production from all three processes are enhanced. In particular, the effect of decreasing hadron masses on kaon production from the meson-meson annihilation is most significant. In the hydro-chemical model for heavy-ion collisions, we demonstrate that the observed enhancement of kaon yield in high-energy heavy-ion collisions can be explained if the medium effect is included.

Mean-field effects and apparent temperatures of nucleons and antinucleons

V. Koch, G.E. Brown

Physics Department, State University of New York, Stony Brook, NY 11794, USA

and

C.M. Ko

Cyclotron Institute and Physics Department, Texas A&M University, College Station, TX 77843, USA

Received 26 April 1991; revised manuscript received 31 May 1991

It is shown that collective scalar and vector fields may affect particle spectra in heavy-ion collisions at the AGS energies. In model calculations we find that in particular the slope parameter of antiprotons is changed considerably leading to a lower apparent temperature than that of protons in qualitative agreement with preliminary experimental data.

Medium effects on kaon and antikaon spectra in heavy-ion collisions

X. S. Fang and C. M. Ko

Cyclotron Institute and Physics Department, Texas A&M University, College Station, Texas 77843

G. E. Brown and V. Koch

Department of Physics, State University of New York, Stony Brook, New York 11794

(Received 3 November 1992)

In the linear chiral perturbation theory, both kaon and antikaon masses decrease in dense matter. There is also a repulsive vector potential for the kaon and an attractive one for the antikaon. With these effects included in the relativistic transport model, it is found that the slope parameter of the kaon kinetic energy distribution is larger than that of the antikaon. This is consistent with the experimental data from heavy-ion collisions in the Alternating Gradient Synchrotron experiments at Brookhaven.

Enhancement of Low-Mass Dileptons in Heavy Ion Collisions

G. Q. Li,¹ C. M. Ko,¹ and G. E. Brown²

¹*Cyclotron Institute and Physics Department, Texas A&M University, College Station, Texas 77843*

²*Department of Physics, State University of New York, Stony Brook, New York 11794*

(Received 24 April 1995; revised manuscript received 14 July 1995)

Using a relativistic transport model for the expansion stage of S + Au collisions at 200 GeV/nucleon, we show that the recently observed enhancement of low-mass dileptons by the CERES Collaboration can be explained by the decrease of vector meson masses in hot and dense hadronic matter.

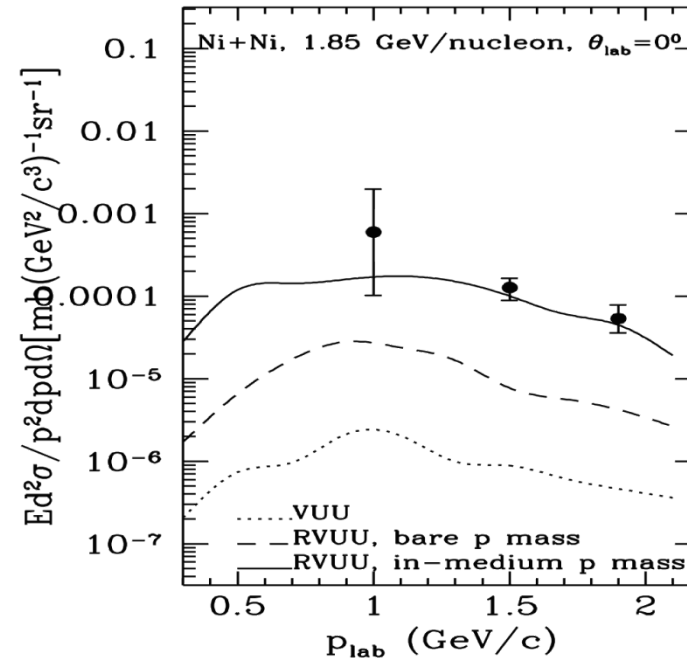
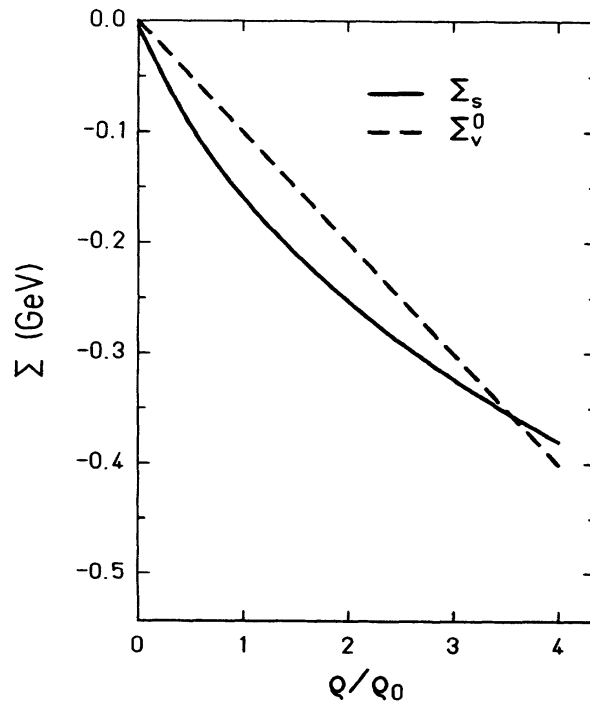
Hadronic potentials in nuclear medium (I)

Ko & Li, JPG 22, 1673 (1996); Ko,
Koch & Li, ARNPS 47, 505 (1997)

- **Nucleons and antinucleons:** Relativistic mean-field model → attractive scalar potential Σ_s and repulsive vector potential Σ_v (“+” for nucleons and “-” for antinucleons due to G-parity)

$$U_{N,\bar{N}}(\rho_s, \rho_B) = \Sigma_s(\rho_s, \rho_B) \pm \Sigma_v^0(\rho_s, \rho_B) = \frac{g_\sigma^2}{m_\sigma^2} \rho_s \pm \frac{g_\omega^2}{m_\omega^2} \rho_B$$

$$U_N = -60 \text{ MeV}, U_{\bar{N}} = -260 \text{ MeV at } \rho_0 = 0.16 \text{ fm}^{-3}$$



- Deep antiproton attractive potential reduces its production threshold and thus enhances its yield in subthreshold heavy ion collisions.

Hadronic potentials in nuclear medium (II)

Ko & Li, JPG 22, 1673 (1996); Ko,
Koch & Li, ARNPS 47, 505 (1997)

- **Kaons and antikaons:** Chiral effective Lagrangian → repulsive potential for kaons and attractive potential for antikaons

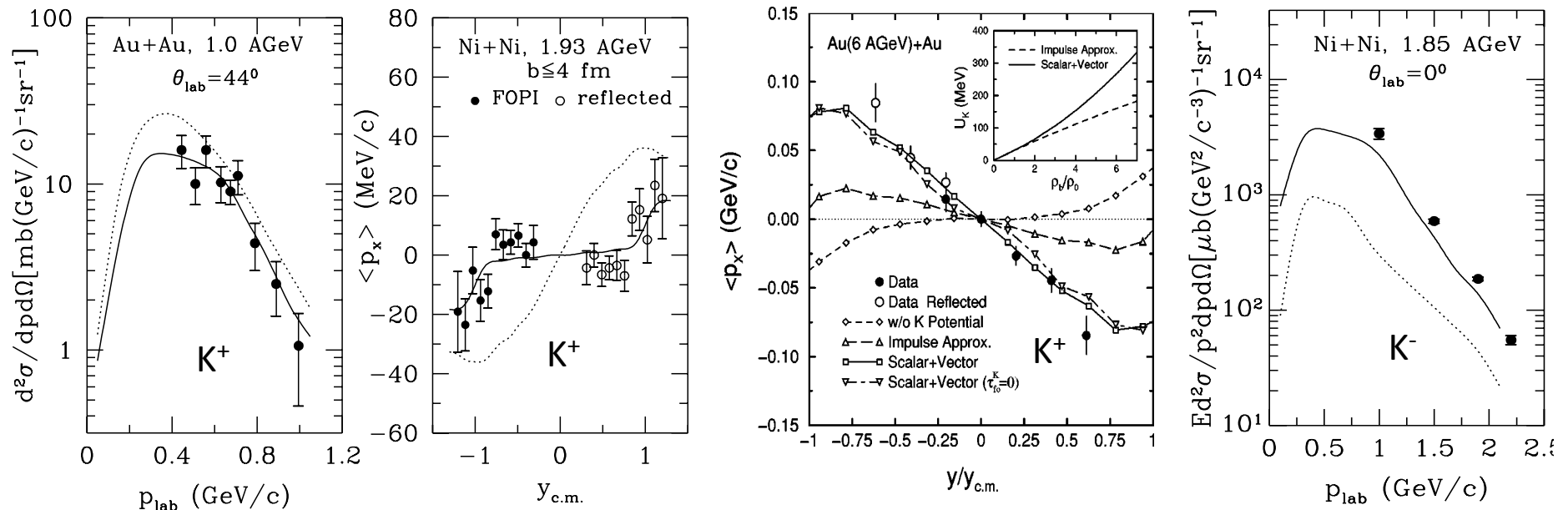
$$U_{K,\bar{K}} = \omega_{K,\bar{K}} - \omega_0, \quad \omega_0 = \sqrt{m_K^2 + p^2}$$

$$\omega_{K,\bar{K}} = \sqrt{m_K^2 + p^2 - a_{K,\bar{K}}\rho_s + (b_K\rho_B)^2} \pm b_K\rho_B$$

$$a_K = 0.22 \text{ GeV}^2 \text{fm}^3, \quad a_{\bar{K}} = 0.45 \text{ GeV}^2 \text{fm}^3$$

$$b_K = 0.33 \text{ GeV}^2 \text{fm}^3$$

$$\Rightarrow U_K = 20 \text{ MeV}, U_{\bar{K}} = -120 \text{ MeV at } \rho_0 = 0.16 \text{ fm}^{-3}$$

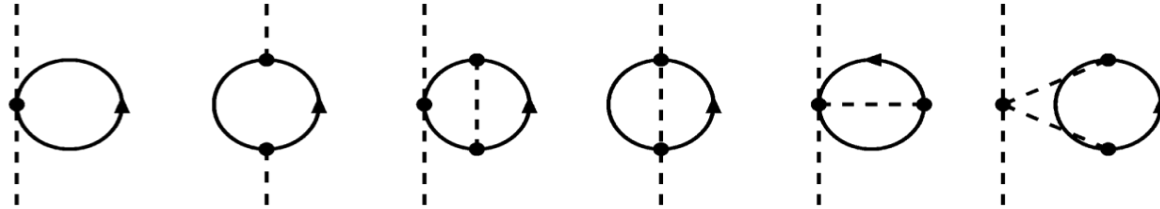


- Experimental data on spectrum and directed flow are consistent with repulsive kaon and attractive antikaon potentials.

Hadronic potentials in nuclear medium (III)

Kaiser & Weise,
PLB 512, 283 (2001)

- **Pions:** $U_{\pi} = \Pi / (2m_{\pi})$ in terms of pion selfenergies



$$\Pi^{-}(\rho_n, \rho_p) = \rho_n [T_{\pi N}^{-} - T_{\pi N}^{+}] - \rho_p [T_{\pi N}^{-} + T_{\pi N}^{+}] + \Pi_{\text{rel}}^{-}(\rho_n, \rho_p) + \Pi_{\text{cor}}^{-}(\rho_n, \rho_p)$$

$$\Pi^{+}(\rho_p, \rho_n) = \Pi^{-}(\rho_n, \rho_p)$$

$$\Pi^0(\rho_n, \rho_p) = -(\rho_p + \rho_n)T_{\pi N}^{+} + \Pi_{\text{cor}}^0(\rho_n, \rho_p)$$

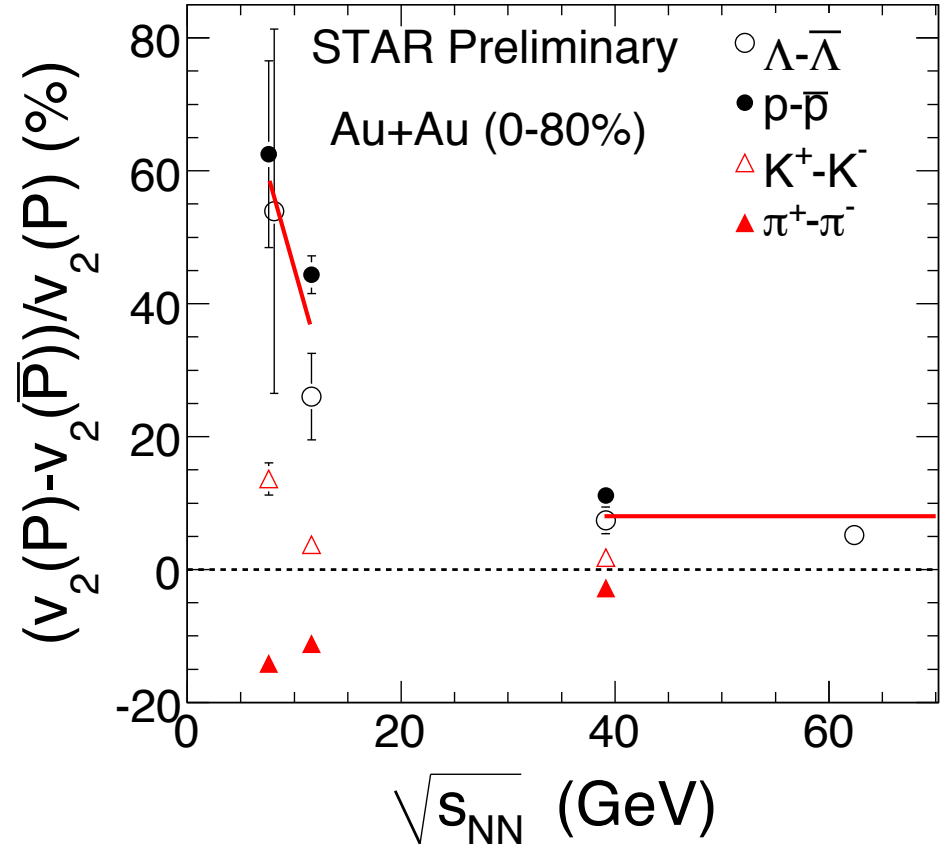
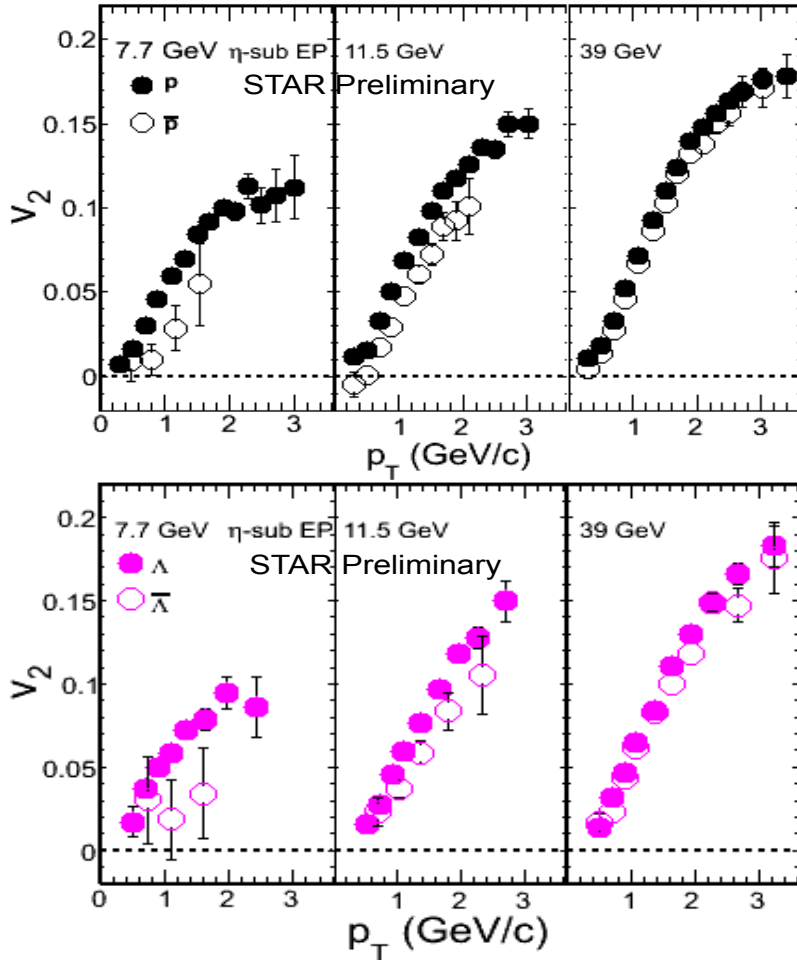
Isospin even and odd πN -scattering matrices extracted from energy shift and width of 1s level in pionic hydrogen atom

$$T_{\pi N}^{+} \approx 1.847 \text{ fm} \quad \text{and} \quad T_{\pi N}^{-} \approx -0.045 \text{ fm}$$

At normal nuclear density $\rho = 0.165 \text{ fm}^{-3}$ and isospin asymmetry $\delta = 0.2$ such as in Pb,

$$U_{\pi^{-}} = 14 \text{ MeV}, \quad U_{\pi^{+}} = -1 \text{ MeV}, \quad U_{\pi^0} = 6 \text{ MeV}$$

Particle and antiparticle elliptic flows at RHIC



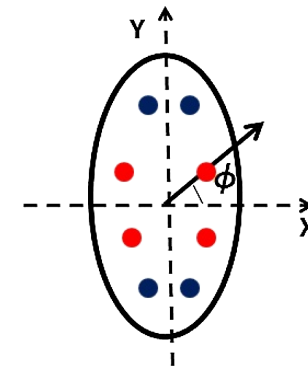
- Particle and antiparticle elliptic flows become significantly different below $\sqrt{s_{NN}} < 11.5$ GeV: $v_2(\text{baryon}) > v_2(\text{anti-baryon})$, $v_2(K^+) > v_2(K^-)$, and $v_2(\pi^+) < v_2(\pi^-)$.
- p_T -integrated relative v_2 difference between particles and antiparticles: **63%**, 44%, and 12% for (p , \bar{p}), **53%**, 25%, and 7% for (Λ , $\bar{\Lambda}$), **13%**, 3%, and 1% for (K^+ , K^-), **-15%**, -10%, and -3% for (π^+ , π^-) at **7.7**, 11.5, and 39 GeV.

Possible explanations for different particle and antiparticle elliptic flows

- **Chiral magnetic wave** [Bumier, Kharzeev, Liao & Yee, PRL 107, 052303 (2011)]

- Stemming from the coupling of the density waves of electric and chiral charge induced by the axial anomaly in the presence of an external magnetic field

$$j_V = \frac{N_c e}{2\pi^2} \mu_A B, \quad j_A = \frac{N_c e}{2\pi^2} \mu_V B$$



- Electric quadrupole moment in QGP
- radial flow leads to decreasing positive hadron and increasing negative hadron elliptic flows
- $v_2(\pi^+) < v_2(\pi^-)$

- Effects on p and \bar{p} as well as K^+ and K^- are masked by different absorption cross sections

- **Transport versus produced particles** [Dunlop, Lisa & Sorensen, PRC 84, 044914 (2011)]: Larger elliptic flow for transport than for produced (anti)particles

- **Different particle and antiparticle transport coefficients** [Greco, Mitrovski & Torrieri, PRC 86, 044905 (2012)] : Large absorption cross sections for antiparticles

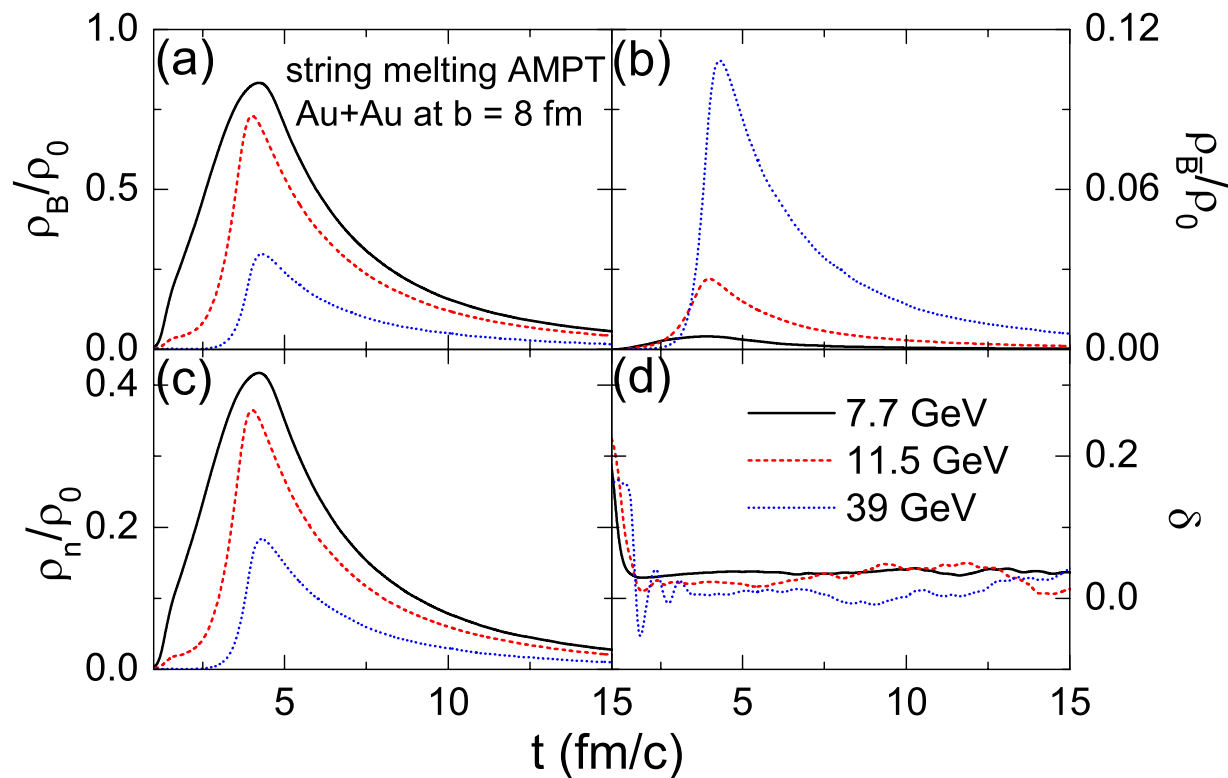
- **Baryon charge, strangeness and isospin conservations** [Steinheimer, Koch & Bleicher, PRC 86, 044903 (2012)]: Decreasing pbar/p ratio with radial distance

- **Different particle and antiparticle potentials** [Xu, Chen, Lin & Ko, PRC 85, 041901(R) (2012)]: Repulsive potential for particles and attractive potential for antiparticles

- **Different quark and antiquark potentials** [Song, Plumari, Greco, Ko & Li, arXiv:1211.5511 [nucl-th]]: Repulsive vector potential for quarks and attractive one for antiquarks

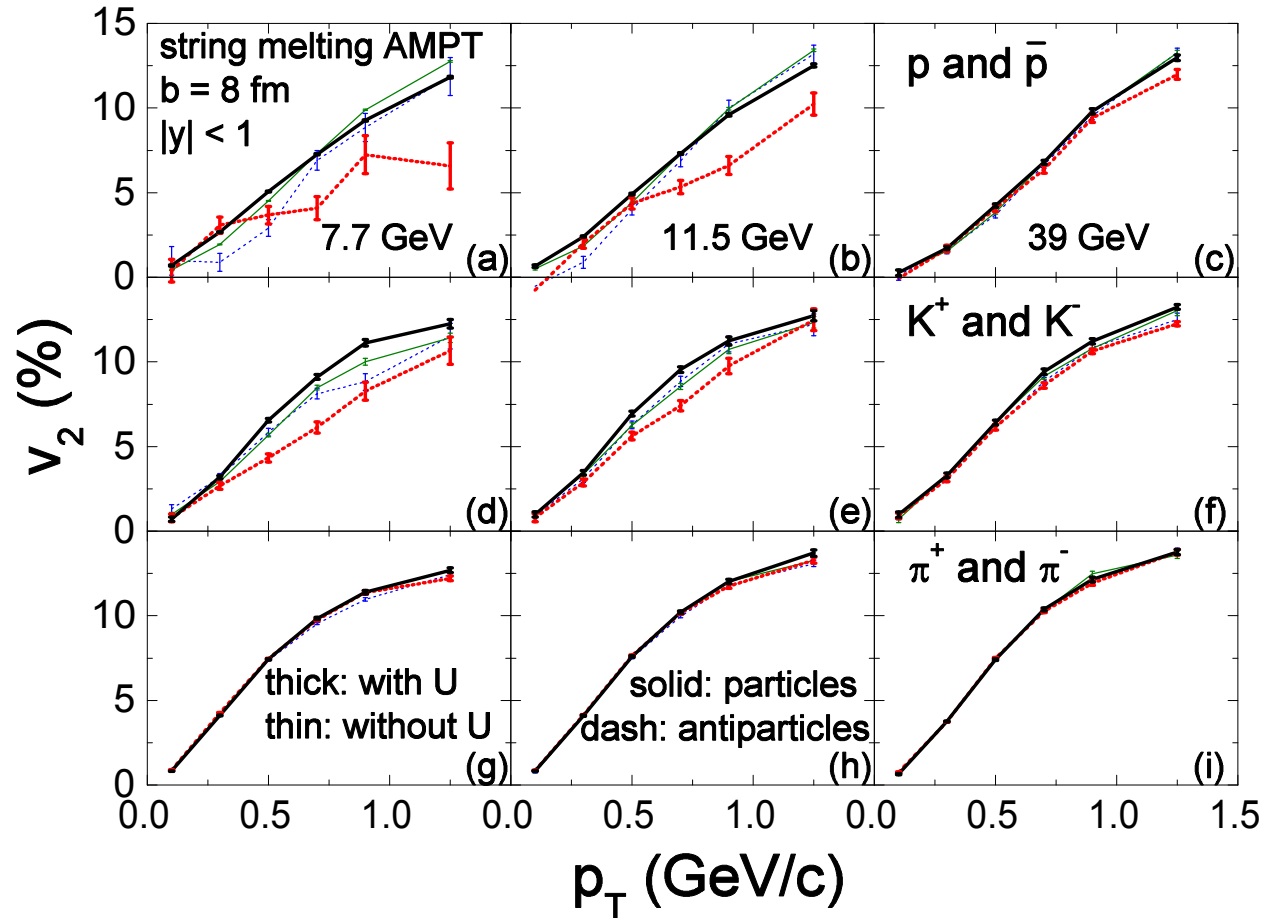
Hadron density evolutions in AMPT

Adjusting parton scattering cross section and ending time of partonic stage to approximately reproduce measured elliptic flows and extracted hadronic energy density ($\sim 0.35 \text{ GeV/fm}^3$): isotropic cross sections of **3**, 6 and 10 mb, and parton ending time of **3.5**, 2.6, 2.9 fm/c for $s^{1/2}_{\text{NN}} = \text{7.7}$, 11.5, and 39 GeV, respectively



- Increasing baryon and decreasing antibaryon densities with decreasing energy
- Increasing neutron density with decreasing energy, but small isospin asymmetry ($\delta=0.02$) due to production of Λ hyperon and pions

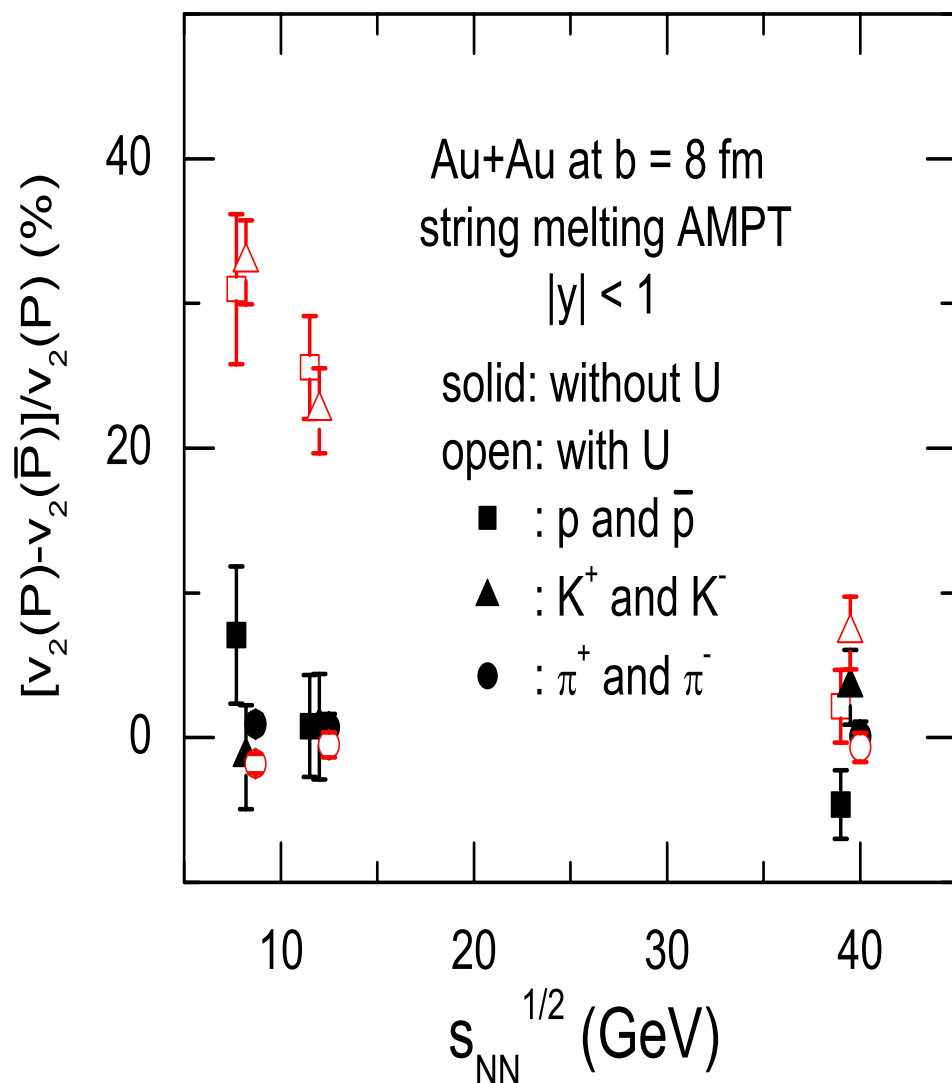
Particle and antiparticle differential elliptic flows



- Similar particle and antiparticle elliptic flows without hadronic potentials.
- Hadronic potentials increase slightly p and pbar v_2 at $p_T < 0.5$ GeV but reduce slightly (strongly) p (pbar) v_2 at high p_T .
- Hadronic potentials increase slightly v_2 of K^+ and reduce v_2 of K^- .
- Effects of hadronic potentials on π^+ and π^- v_2 are small.

P_T-integrated particle and antiparticle elliptic flow difference

Xu, Chen, Ko & Lin, PRC 85, 045905 (2012)

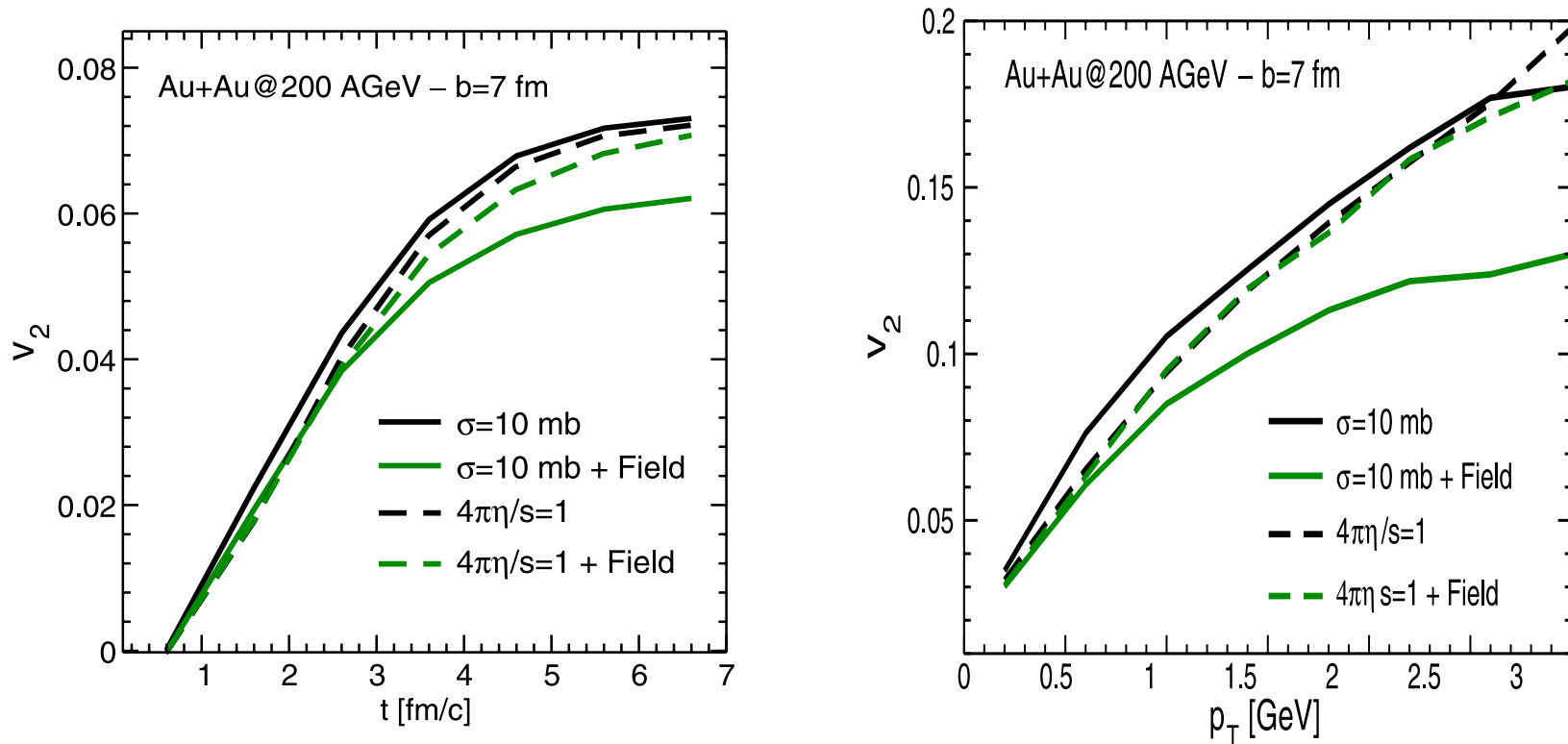


→ Hadronic potentials underestimate p - \bar{p} and overestimate K^+ - K^- v_2 difference

- Difference very small without hadronic potentials → different particle and antiparticle scattering and absorption cross sections have small effects.
- Hadronic potentials lead to relative v_2 difference between p and \bar{p} and between K^+ and K^- of **30%** at 7.7 GeV, 20% at 11.5 GeV, and negligibly small value at 39 GeV, only very small negative value between π^+ and π^- .
- Compared to experimental values of **63%**, 44%, and 12% for (p, \bar{p}) , **13%**, 3%, and 1% for (K^+, K^-) , **-15%**, -10%, and -3% for (π^+, π^-) at 7.7, 11.5, and 39 GeV, ours are smaller for (p, \bar{p}) and (π^+, π^-) and larger for (K^+, K^-) .

Effects of attractive scalar potential in quark matter

Plumari, Baran, Di Tori, Ferini, and Greco, PLB 689, 18 (2010)



- Attractive scalar potential reduces v_2 of both quark and antiquark.
- Effects are reduced when parton scattering cross section is large.

Quark and antiquark potentials in QGP (I)

- NJL model [Bratovic, Hatsuda & Weise, PLB 719, 131 (2013)]

$$\begin{aligned} \mathcal{L} = & \bar{\psi}(i \not{\partial} - M)\psi + \frac{G}{2} \sum_{a=0}^8 \left[(\bar{\psi} \lambda^a \psi)^2 + (\bar{\psi} i \gamma_5 \lambda^a \psi)^2 \right] && \text{Scalar-pseudoscalar} \\ & + \sum_{a=0}^8 \left[\frac{G_V}{2} (\bar{\psi} \gamma_\mu \lambda^a \psi)^2 + \frac{G_A}{2} (\bar{\psi} \gamma_\mu \gamma_5 \lambda^a \psi)^2 \right] && \text{Vector-axial vector} \\ & - K \left[\det_f \left(\bar{\psi} (1 + \gamma_5) \psi \right) + \det_f \left(\bar{\psi} (1 - \gamma_5) \psi \right) \right], && \text{Kobayashi-Maskawa-} \\ & && \text{t'Hooft (KMT)} \end{aligned}$$

where $\det_f(\bar{\psi} \Gamma \psi) = \sum_{i,j,k} \varepsilon_{ijk} (\bar{u} \Gamma q_i) (\bar{d} \Gamma q_j) (\bar{s} \Gamma q_k).$

- Mean-field approximation

$$\mathcal{L} = \bar{\psi} \left(i \partial^\mu - \frac{2}{3} G_V \langle \bar{\psi} \gamma^\mu \psi \rangle \right) \gamma_\mu \psi - \bar{\psi} M^* \psi + \dots$$

where $M^* = \text{diag}(M_u, M_d, M_s)$ with

$$\begin{aligned} M_u &= m_u - 2G \langle \bar{u} u \rangle + 2K \langle \bar{d} d \rangle \langle \bar{s} s \rangle & \langle \bar{q}_i q_i \rangle &= -2M_i N_c \int \frac{d^3 \mathbf{k}}{(2\pi)^3 E_i} [1 - f_i(k) - \bar{f}_i(k)] \\ M_d &= m_d - 2G \langle \bar{d} d \rangle + 2K \langle \bar{s} s \rangle \langle \bar{u} u \rangle & & \\ M_s &= m_s - 2G \langle \bar{s} s \rangle + 2K \langle \bar{u} u \rangle \langle \bar{d} d \rangle & \langle \bar{\psi} \gamma^\mu \psi \rangle &= 2N_c \sum_{i=u,d,s} \int \frac{d^3 \mathbf{k}}{(2\pi)^3 E_i} k^\mu [f_i(k) - \bar{f}_i(k)], \end{aligned}$$

Quark and antiquark potentials in QGP (II)

$$U_{q,\bar{q}} = \sqrt{M_q^2 + (\vec{p} \mp g_v \vec{\rho})^2} \pm g_v \rho_0 - \sqrt{m_q^2 + \vec{p}^2}$$

$$\text{Net baryon current: } \vec{\rho} = \langle \bar{\psi} \vec{\gamma} \psi \rangle \quad g_v = \frac{2}{3} G_V$$

$$\text{Net baryon density: } \rho_0 = \langle \bar{\psi} \gamma^0 \psi \rangle$$

- Quark mass is modified by the quark condensate
 - attractive scalar potential on both quark and antiquark
- Vector potential is repulsive for quark and attractive for antiquark
 - enhances relative v_2 difference between quarks and antiquarks
 - enhances relative v_2 difference between p and pbar, Λ and Λ bar, K^+ and K^-

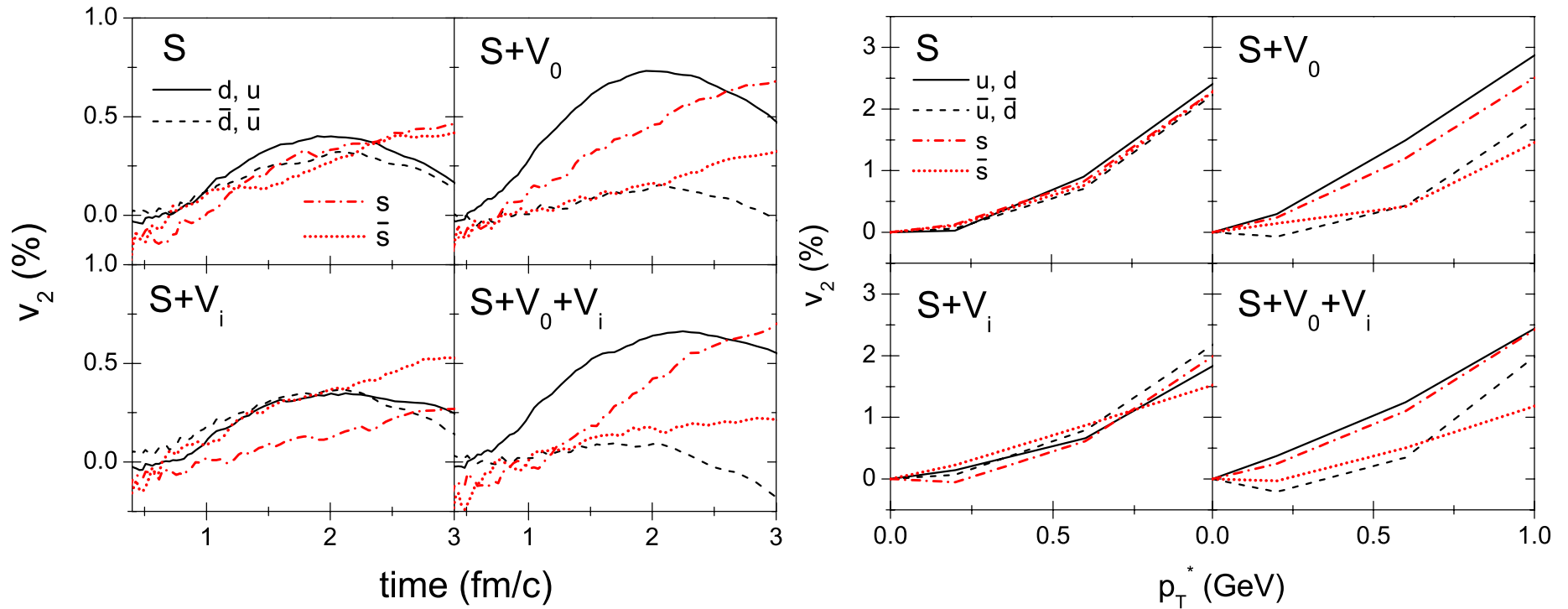
→ Would bring results with only hadronic potentials closer to experimental data

Effects of vector potential in quark matter

Song, Plumari, Greco, Ko & Li,
arXiv:1211.5511

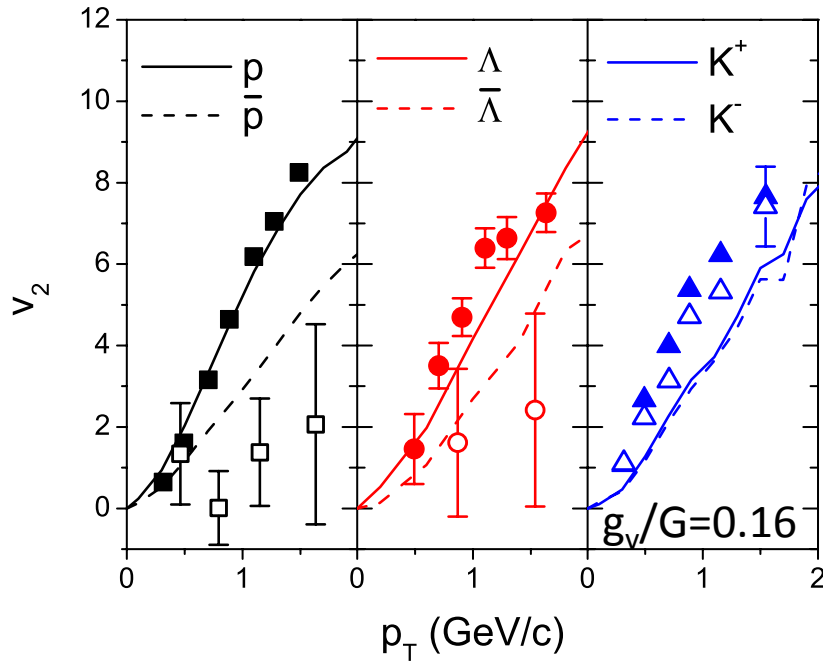
Using $m_u = m_d = 3.6$ MeV, $m_s = 87$ MeV, $G\Lambda^2 = 3.6$, $K\Lambda^5 = 8.9$, $\Lambda = 750$ MeV

Initial parton distributions from AMPT

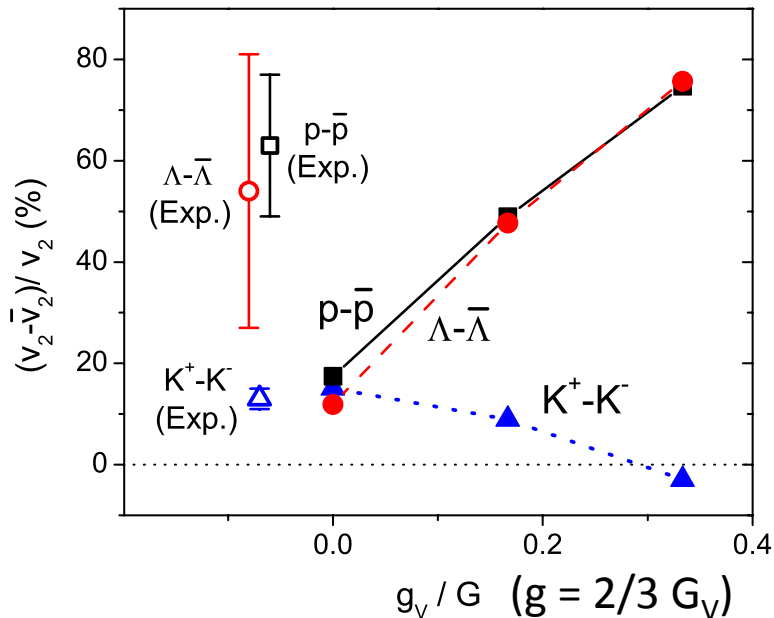


- Time (electric) component of vector potential increases quark but decreases antiquark elliptic flows.
- Space (magnetic) component of vector potential has a similar effect at low p_T but an opposite effect at high p_T .
- Net effect of vector potential: larger quark than antiquark elliptic flows.

Partonic mean-field effects on hadron and antihadron v_2



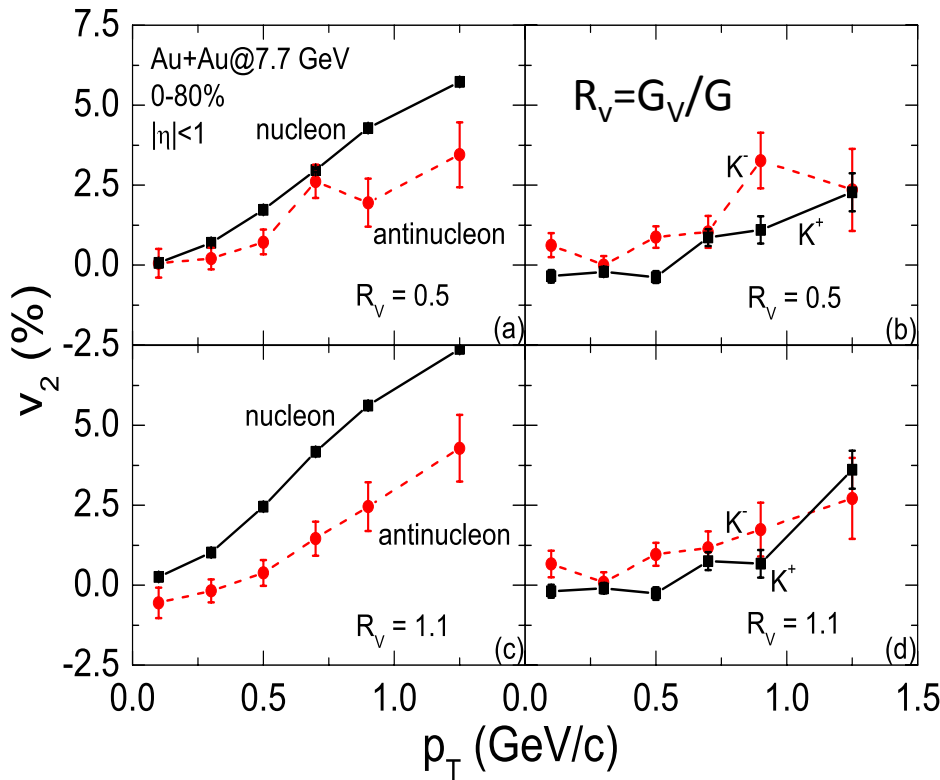
- Using recombination (coalescence) model to produce hadrons (proton, lambda, kaon) and their antiparticles from quarks and antiquarks at hadronization.
- Smaller antiquark than quark v_2 leads to smaller v_2 for antiproton than proton, antilambda than lambda, and K^- than K^+ .



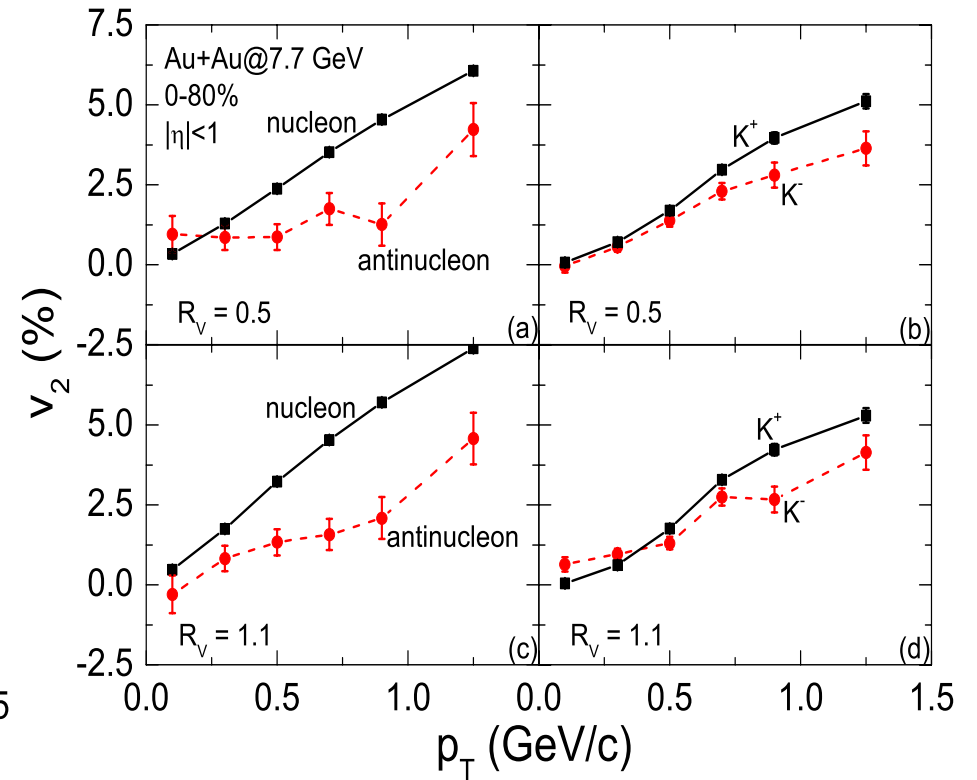
- Relative v_2 differences between proton and antiproton, lambda and antilambda, increase almost linearly with the strength of quark vector interaction.
- Relative v_2 difference between K^+ and K^- decreases with the strength of quark vector interaction.

Effects of hadronic evolution (mean fields + scattering)

Jun, Song, Ko & Li, arXiv:1308:1753;
PRL, in press

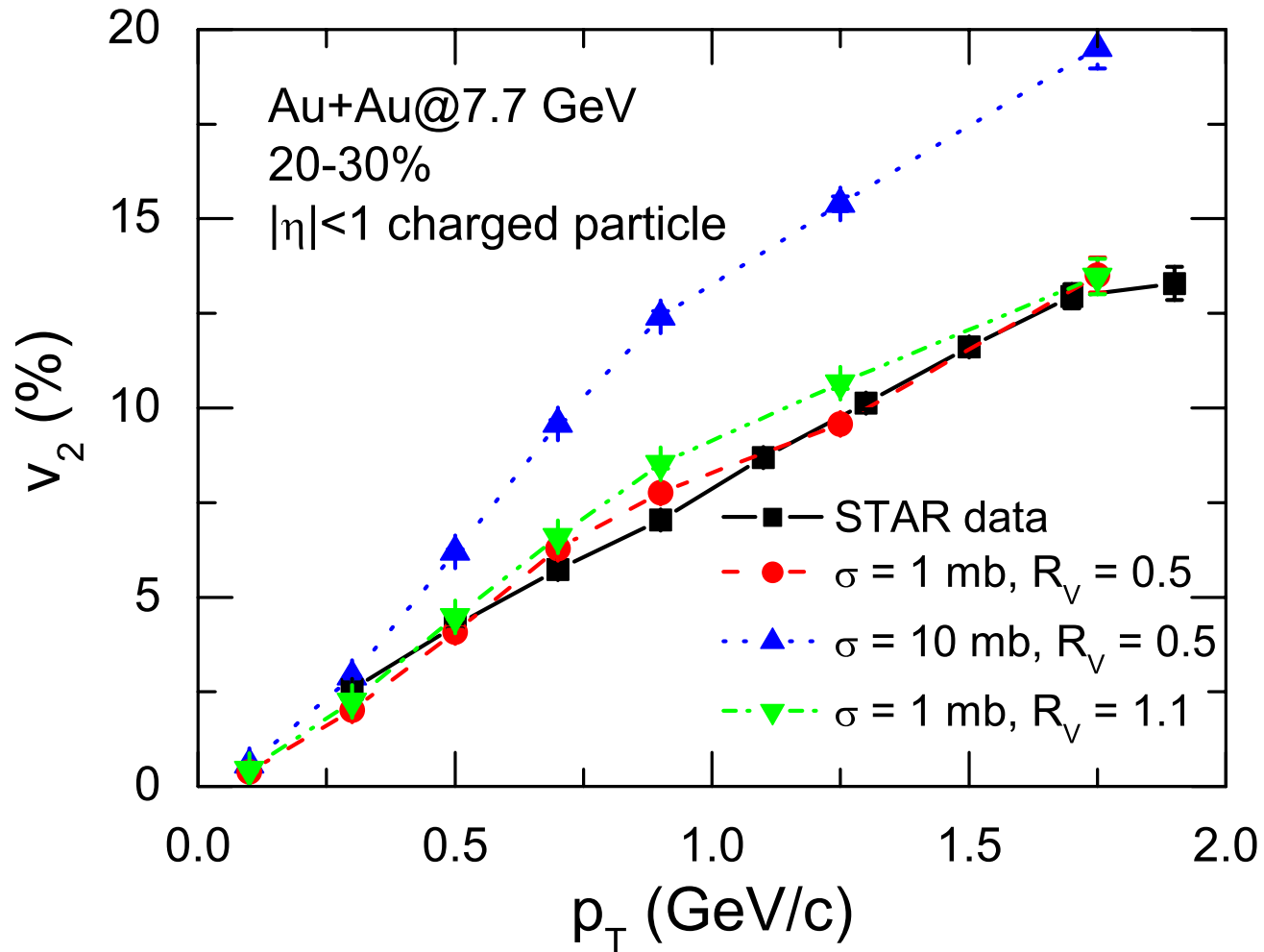


- Before hadronic evolution
 - nucleons have larger v_2 than antinucleons
 - K^- have larger v_2 than K^+



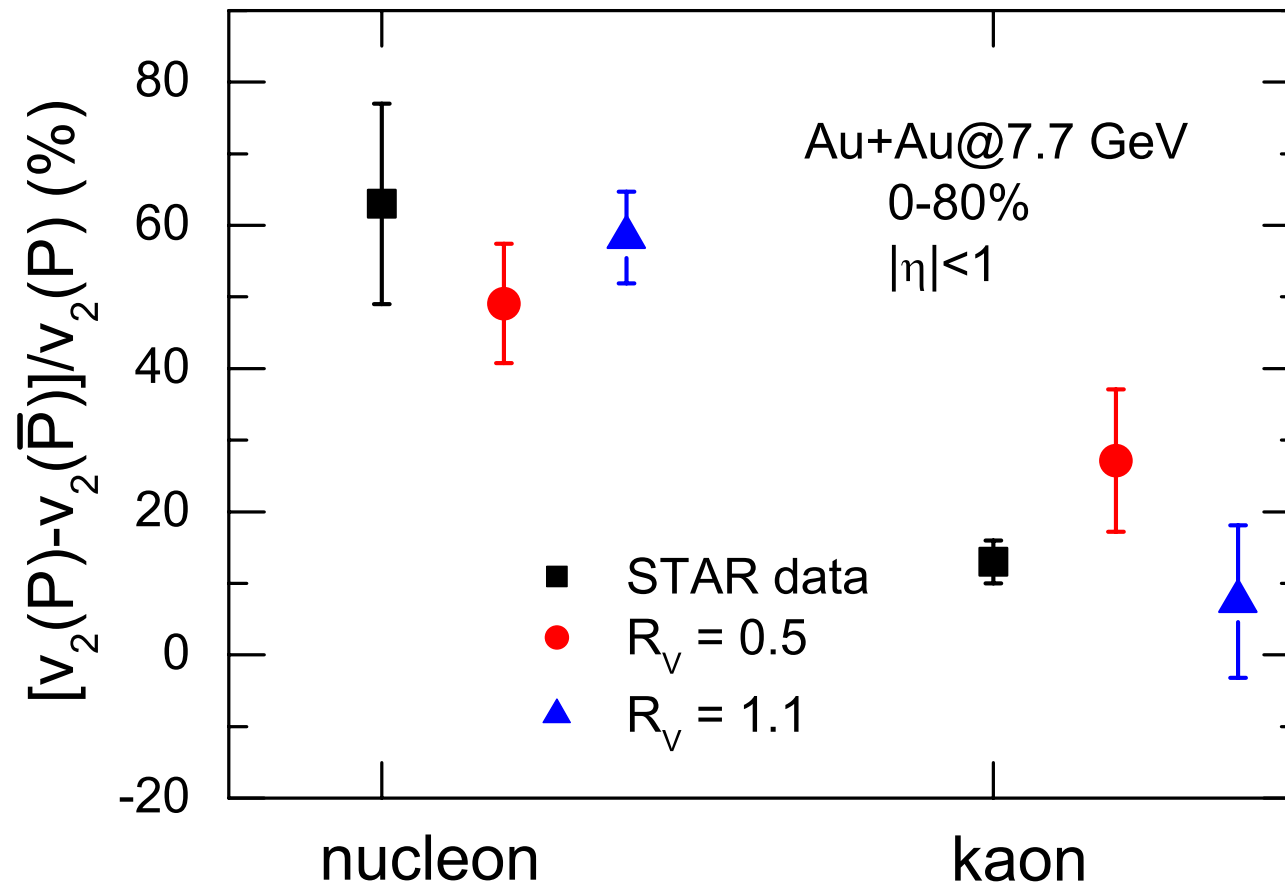
- After hadronic evolution
 - v_2 increases for all hadrons
 - v_2 of nucleons remains larger than that of antinucleons
 - v_2 of K^+ becomes larger than that of K^-

Charged hadron elliptic flow



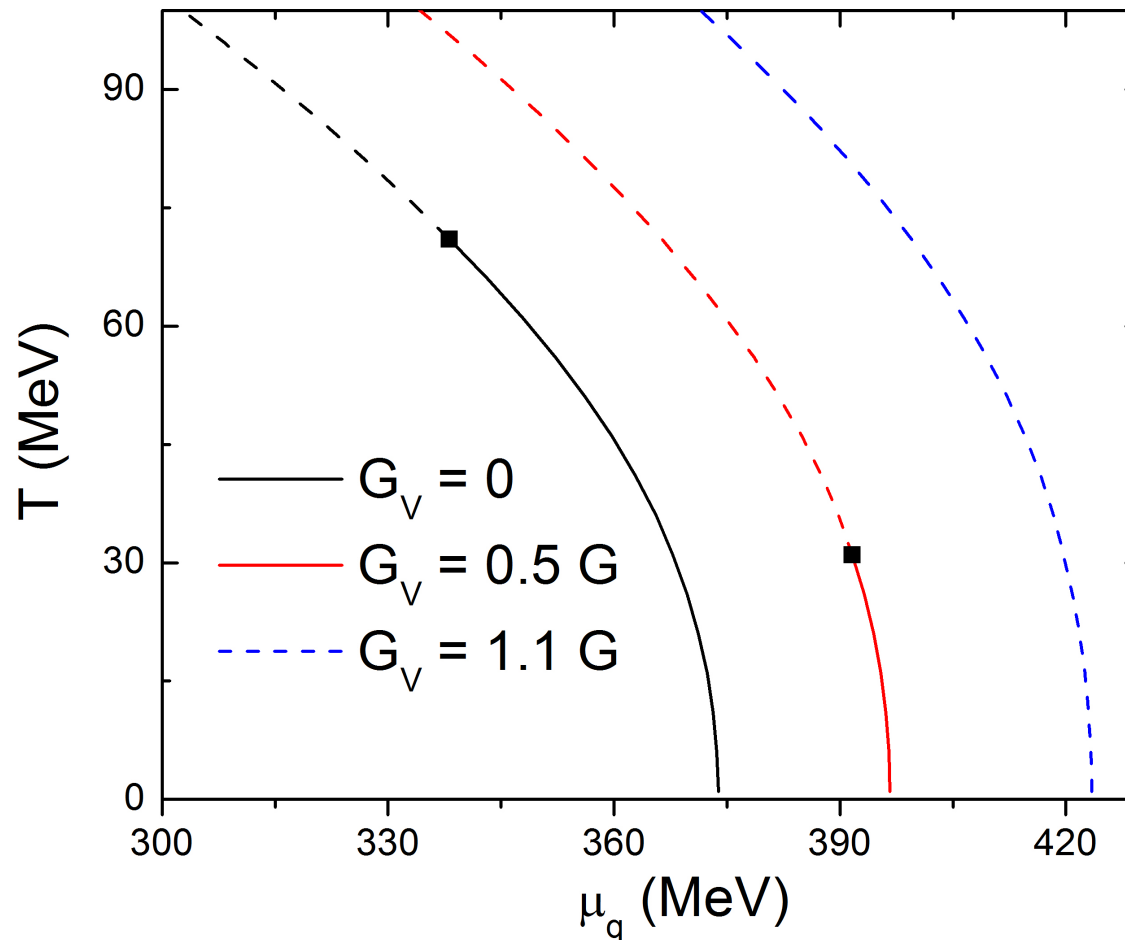
- Sensitive to parton cross section \rightarrow 1 mb to reproduce data
- Insensitive to partonic vector mean fields

Relative v_2 difference including both partonic and hadronic potentials



- Finite partonic vector mean field with $G_V/G=0.5-1.1$ is needed to describe STAR data.

Effects of vector interaction on QCD phase diagram



- Location of critical point depends strongly on G_V ; moving to lower temperature and larger baryon chemical potential as G_V increases.
- Critical point disappears for $G_V > 0.6 G$.

Summary

- Different particle and antiparticle v_2 is observed in BES at RHIC where produced matter has a large finite baryon chemical potential (~ 400 MeV).
- Taking into account different potentials for hadrons and antihadrons can partially account for the experimental observation.
- Quarks and antiquarks are affected by scalar and vector potentials in QGP,
 - reduced v_2 due to attractive scalar potential
 - vector potential becomes nonzero at finite baryon chemical potential; repulsive for quarks and attractive for antiquarks
 - larger quark than antiquark v_2 in baryon-rich QGP
 - larger v_2 for proton than antiproton, lambda than antilambda, and K^+ than K^- (small G_V) or K^- than K^+ (large G_V) after hadronization
- Including both partonic and hadronic potentials $\rightarrow G_V = 0.5 - 1.1$ G \rightarrow absence of critical point in QCD phase diagram?
- Information on quark and antiquark potentials at finite baryon chemical potential is useful for understanding the phase structure of QCD.
- Gerry would be very happy to know that mean-field effects also play important roles in HIC at RHIC.